A Phenomenological Two-Dimensional Model of Constrained Recovery in Shape Memory Alloy Rings

T. VIDENIC, F. KOSEL, A. PUKSIC and M. BROJAN
Department of Mechanics
Faculty of Mechanical Engineering, University of Ljubljana
Askerceva 6, 1000 Ljubljana
SLOVENIA
tomaz.videnic@fs.uni-lj.si http://www.fs.uni-lj.si/lanem

Abstract: - In this article constrained recovery in a thick-walled shape memory alloy (SMA) ring with a rectangular cross section is modeled using the theory of generalized plasticity. As a mechanical obstacle that delays free recovery in a SMA ring, a steel ring is used. The result of constrained recovery is generation of high stresses in both rings. All equations are written in a closed form in terms of infinite series. Theoretical results are compared with experimental results and good agreement is found when SMA rings are in the domain of recoverable strains.

Key-Words: - shape memory alloys, rings, constrained recovery, generalized plasticity

1 Introduction

Shape memory alloys (SMA) have an intrinsic capacity to return to a previously defined shape by increasing the alloy's temperature. This effect arises from reversible and rate-independent martensitic transformation and resulting changes of crystal structure of the solid phases of the material. A low-temperature phase is called martensite and a high one is austenite. Large residual strains of even 10% can be recovered in this way and the process is often refered as free recovery. The return to the original shape begins at a temperature called austenite start temperature A_S, and completes at the austenite finish temperature A_f. If the free recovery is hampered by an external obstacle before temperature A_f is reached, the process is called constrained recovery and large stresses, can be generated in SMA elements. This property makes SMA ideally suited for use as fasteners, seals, connectors and clamps [1,2].

The principal aim of the present paper is to develop a phenomenological model of the biaxial constrained recovery in SMA rings, using the generalized plasticity theory [3-6]. Available publications on the process of constrained recovery are mostly limited only to uniaxial examples [7-14] which is unusual because some of the most successful applications of the SMA to date are tube couplings [15]. To the authors' knowledge, a mathematical model of biaxial constrained recovery in SMA rings is still missing.

In our study, a ring made of an ordinary steel material is used as a mechanical obstacle which delays free recovery in an $Ni_{48}Ti_{38}Nb_{14}$ SMA ring. Theoretical results are compared with experimental findings. Six commercial SMA rings were subjected to constrained recovery and one SMA ring was heated without a mechanical obstacle (free recovery) in order to get the data for parameters α and λ_M, which are needed in the phenomenological model.

2 The process of constrained recovery

The entire process of constrained recovery can be represented in six steps: (1) An SMA ring is cooled from austenite to multi-variant martensite at zero stress. (2) The SMA ring is widened in a martensitic region (stress-induced or oriented martensite) at a constant temperature. (3) The SMA ring and ordinary steel ring are then heated, and until temperature A_S is reached both elements extend. (4) At temperature A_S the SMA ring starts to contract, while the ordinary ring still extends until at temperature T_C both elements touch each other and the process of constrained recovery in the SMA ring begins. (5) Above temperature T_C, retransformation to austenite is constrained and continues until temperature T_{SE} at which the retransformation in the SMA ring is completed. The stresses in the SMA ring increase, therefore temperature T_{SE} is considerably higher than A_f. (6) Both rings are cooled down to the end temperature T_{END}, which can be equal to the ambient temperature T_0, and are still in contact. Since temperature $M_S(\sigma_e)$ is lower than T_0, the transformation from austenite to martensite and consequently relaxation of stresses in the SMA ring does not begin.

The first two steps will not be dealt with here, since commercial $Ni_{48}Ti_{38}Nb_{14}$ SMA rings in the widened 'ready to use' martensitic state are available

from "Intrinsic Devices Inc." The analysis of the third and fourth step is simple and will also be ommited because of the lack of the space. It can be found elsewhere [16]. The geomety of both rings in different temperature regions is shown in Fig. 1.

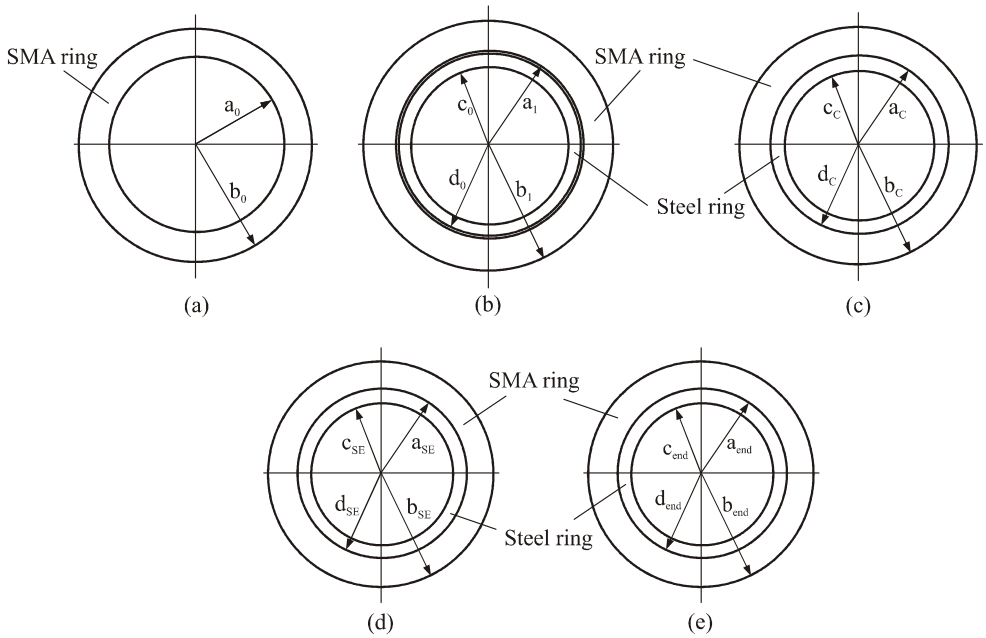

Fig. 1. Geometry of both rings at different temperatures: (a) Before stretching of the SMA ring in martensitic state at constant temperature inner and outer radius are a_0 and b_0. (b) Geometry of both rings at ambient temperature T_0 after stretching and unloading of the SMA ring. The SMA ring is in martensitic and widened state $a_1 > d_0 > a_0$. (c) At temperature T_C the rings touch each other. (d) In the SMA ring transformation to austenite is finished at temperature T_{SE}. Large stresses occur in both rings. (e) Rings are cooled down to the end temperature T_{END}, which can be equal to the temperature T_0.

3 Modelling of constrained recovery

In a two phase system (martensite and austenite), it can be assumed that the only internal variable is the fraction of mass occupied by one of the phases. In SMA models this variable is usually the mass fraction of martensite ξ, with $\xi = 0$ denoting all austenite and $\xi = 1$ all martensite. A single internal variable model is suitable for modelling constrained recovery since there is no conversion between martensite variants. In the region where phase transformation from martensite to austenite may take place a stress decrease at constant temperature, a temperature increase at constant stress or a proper combination of these actions should occur. Using the generalized plasticity theory, the linear flow rule can be written:

$$\xi(r;T) = \xi_0(r)\frac{\sigma_e(r;T) - C(T - A_f)}{C(A_f - A_S)} \tag{1}$$

where r is the radius of the SMA ring, ξ_0 is initial mass fraction of the martensite at the beginnig of the phase transformation, σ_e is the effective stress in the SMA ring and C is stress rate. In the case of constrained recovery in a SMA ring only two components of a stress tensor are not equal to zero: normal radial stress σ_r and normal circular stress σ_φ. If $\sigma_\varphi \geq 0$ and $\sigma_r \leq 0$, the effective stress can be defined in the next form:

$$\sigma_e = \sigma_\varphi - \sigma_r + \alpha(\sigma_r + \sigma_\varphi) \tag{2}$$

where α is the measure of unequal response in tension and compression and should be determined experimentally. The special case $\alpha = 0$ corresponds to equal response; the effective stress σ_e is then of Tresca type. The strain tensor ε_{ij} in SMA can be divided in two parts:

$$\varepsilon_{ij} = \varepsilon_{ij}^{el}(\sigma_{ij};T) + \varepsilon_{ij}^{iel}(\xi) \tag{3}$$

where ε_{ij}^{el} is elastic part and ε_{ij}^{iel} inelastic part of the strain tensor. Recoverable strains during martensite phase transformation can be described by the inelastic strain tensor:

$$\varepsilon_{ij}^{iel} = \lambda_M \xi \frac{\partial \sigma_e}{\partial \sigma_{ij}} \tag{4}$$

where λ_M is a constant which must be determined experimentally. In steel ring are assumed elastic strains during the whole process. The contact temperature T_C

can be calculated from the condition of equal radii a_C and d_C, Fig. 1c:

$$T_C = \frac{\left[\left(1-\alpha_{st}T_0\right)d_0 - \left(1+\alpha_S T_0\right)a_0\right]\left(A_f - A_S\right) - \lambda_M\left(1+\alpha\right)A_f a_0}{\left(\alpha_S a_0 - \alpha_{st} d_0\right)\left(A_f - A_S\right) - \lambda_M\left(1+\alpha\right)a_0} \tag{5}$$

with α_{st} and α_S linear thermal expansion coefficients of the steel and SMA ring respectively. >From the temperature T_C onwards the process of constrained recovery in the SMA ring starts and will be described here more in detail.

3.1 Temperature region $T_C \le T \le T_{SE}$

During the process of constrained recovery the relation between radial and circular strain, displacement u and stresses in the SMA ring can be written from (2-4):

$$\begin{cases} \varepsilon_r = \dfrac{\partial u}{\partial r} = \lambda_M\left(\alpha-1\right)\xi + \alpha_S\left(T-T_0\right) \\ \qquad\qquad + \dfrac{1}{E_S}\left(\sigma_r^{el} - \nu_S\sigma_\varphi^{el}\right) \end{cases} \tag{6}$$

$$\begin{cases} \varepsilon_\varphi = \dfrac{u}{r} = \lambda_M\left(1+\alpha\right)\xi + \alpha_S\left(T-T_0\right) \\ \qquad\qquad + \dfrac{1}{E_S}\left(\sigma_\varphi^{el} - \nu_S\sigma_r^{el}\right) \end{cases} \tag{7}$$

with E_S and ν_S Young's modulus and Poisson's ratio of the SMA ring respectively. It must be noted that elastic stresses σ_r^{el} and σ_φ^{el} are not true stresses (σ_r and σ_φ are true stresses) in the SMA ring. The distinction between σ^{el} and σ originates from theoretical treatment of uniaxial constrained recovery proposed by Rudy Stalmans and his colleagues [11,12]. Using expressions (1) and (2), equilibrium equation $r(\mathrm{d}\sigma_r/\mathrm{d}r) = \sigma_\varphi - \sigma_r$ and after integration with respect to temperature, it can be decuced from (6) and (7):

$$\begin{cases} \left(1+\alpha\right)r\dfrac{\partial^2\sigma_r}{\partial r^2} + \left(1+3\alpha\right)\dfrac{\partial\sigma_r}{\partial r} \\ \qquad = -\dfrac{C^2\left(A_f - A_S\right)a_0^{\frac{2}{1+\alpha}}b_0^2}{\lambda_M\left(1+\alpha\right)E_S}\left[\dfrac{\left(1+\nu_S\right)r^{\frac{1-\alpha}{1+\alpha}}}{b_0^2+\alpha r^2} + \dfrac{\left(1-\alpha-\nu_S\left(1+\alpha\right)\right)r^{\frac{3+\alpha}{1+\alpha}}}{\left(b_0^2+\alpha r^2\right)^2}\right]\left(T-T_C\right) \end{cases} \tag{8}$$

The solution of the above differential equation is:

$$\begin{cases} \sigma_r\left(r;T\right) = -\dfrac{C^2\left(A_f - A_S\right)a_0^{\frac{-2}{1+\alpha}}b_0^2}{2\lambda_M\alpha\left(1+\alpha\right)E_S}\left[\left(1+\nu_S\right)I_2\left(r\right) + \left(1-\alpha-\nu_S\left(1+\alpha\right)\right)I_4\left(r\right)\right]\left(T-T_C\right) \\ \qquad + E_1\left(T\right) + E_2\left(T\right)r^{\frac{-2\alpha}{1+\alpha}} + \dfrac{C^2\left(A_f - A_S\right)a_0^{\frac{-2}{1+\alpha}}b_0^2}{4\lambda_M\alpha^2\left(1+\alpha\right)E_S}\left[\dfrac{1-\nu_S}{\alpha}\ln\dfrac{b_0^2+\alpha r^2}{b_0^2+\alpha a_0^2}\right. \\ \qquad \left. + \dfrac{\left(1-\alpha-\nu_S\left(1+\alpha\right)\right)b_0^2\left(a_0^2-r^2\right)}{\left(b_0^2+\alpha r^2\right)\left(b_0^2+\alpha a_0^2\right)}\right]\left(T-T_C\right)r^{\frac{-2\alpha}{1+\alpha}} \end{cases} \tag{9}$$

with $E_1(T)$ and $E_2(T)$ unknown functions that can be determined from boundary conditions and $I_2(r)$ and $I_4(r)$ integrals which can be solved, using the theorem of Chebyshev, in a closed and infinite form:

$$I_2\left(r\right) = \int_{a_0}^{r}\frac{\rho^{\frac{1-\alpha}{1+\alpha}}}{b_0^2+\alpha\rho^2}d\rho = \frac{1+\alpha}{2}\sum_{k=0}^{\infty}\frac{\left(-\alpha\right)^k\left(r^{2k+\frac{2}{1+\alpha}} - a_0^{2k+\frac{2}{1+\alpha}}\right)}{\left(\left(1+\alpha\right)k+1\right)b_0^{2(k+1)}} \tag{10}$$

$$I_4(r)=\int_{a_0}^{r}\frac{\rho^{\frac{3+\alpha}{1+\alpha}}}{\left(b_0^2+\alpha\rho^2\right)^2}d\rho=\frac{1+\alpha}{2}\sum_{k=0}^{\infty}\frac{(-\alpha)^k(k+1)\left(r^{2k+\frac{4+2\alpha}{1+\alpha}}-a_0^{2k+\frac{4+2\alpha}{1+\alpha}}\right)}{\left((1+\alpha)(k+1)+1\right)b_0^{2(k+2)}} \tag{11}$$

Using the equilibrium equation, circular stress σ_φ in the SMA ring can be determined:

$$\begin{cases}\sigma_\varphi(r;T)=-\dfrac{C^2\left(A_f-A_S\right)a_0^{\frac{-2}{1+\alpha}}b_0^2}{2\lambda_M\alpha(1+\alpha)E_S}\left[(1+\nu_S)I_2(r)+\left(1-\alpha-\nu_S(1+\alpha)\right)I_4(r)\right](T-T_C)\\ \quad+E_1(T)+\dfrac{1-\alpha}{1+\alpha}E_2(T)r^{\frac{-2\alpha}{1+\alpha}}+\dfrac{C^2\left(A_f-A_S\right)(1-\alpha)a_0^{\frac{-2}{1+\alpha}}b_0^2}{4\lambda_M\alpha^2(1+\alpha)^2E_S}\left[\dfrac{1-\nu_S}{\alpha}\ln\dfrac{b_0^2+\alpha r^2}{b_0^2+\alpha a_0^2}\right.\\ \qquad\left.+\dfrac{\left(1-\alpha-\nu_S(1+\alpha)\right)b_0^2\left(a_0^2-r^2\right)}{\left(b_0^2+\alpha r^2\right)\left(b_0^2+\alpha a_0^2\right)}\right](T-T_C)r^{\frac{-2\alpha}{1+\alpha}}\end{cases} \tag{12}$$

There are three boundary conditions. The radial stress at the outer radius of the SMA ring is zero: $\sigma_r(b_0) = 0$. The boundary condition of equal inner radius of the SMA ring and outer radius of the steel ring, $a(T) = d(T)$, is valid during the whole process of constrained recovery. In the second boundary condition the contact radial stress $p_0(T)$ between both rings emerges and additional boundary condition is needed: $\sigma_r(a_0) = -p_0(T)$. In this way, there are three unknowns $E_1(T)$, $E_2(T)$ and $p_0(T)$ and three boundary conditions from which these unknows can be determined. The temperature T_{SE} at which retransformation from martensite to austenite during constrained recovery is completed can be calculated from the equation (1) and the condition $\xi(b_0;T_{SE}) = 0$. When $p_0(T)$ is known, the stress – strain state in the steel ring can easily be determined, since only elastic strains are assumed in it.

3.2 Temperature region $T_{SE} \geq T \geq T_{END}$

The temperature T_{SE} for a commercial $Ni_{48}Ti_{38}Nb_{14}$ SMA ring is usually higher than 100°C. It means that the system SMA ring – steel ring must be cooled down to be used at temperature T_{END}, which is usualy room temperature. In this temperature region, both rings are contracting with decreasing temperature T since transformation from martensite to austenite is finished and transformation from austenite to martensite in the SMA ring has not started yet. Radial and circular strains in the SMA ring can be written:

$$\varepsilon_r=\alpha_S(T-T_{SE})+\frac{1}{E_S}\left(\sigma_r-\nu_S\sigma_\varphi\right) \tag{13}$$

$$\varepsilon_\varphi=\alpha_S(T-T_{SE})+\frac{1}{E_S}\left(\sigma_\varphi-\nu_S\sigma_r\right) \tag{14}$$

where stresses σ_r and σ_φ are true stresses since there is no phase transformation. In the similar way as in the previous temperature region it is possible to write governing differential equation, but will be ommited here because it is more complicated than equation (8) and because of the lack of the space. Boundary conditions are the same as before. The stress state in both rings is very similar as in the previous temperature region since linear thermal expansion coefficients of both materials α_{st} and α_S are similar. Of course, the strain state in the rings is not similar at both temperatures, since rings contract during cooling from T_{SE} to T_{END}.

4 Numerical and experimental results

The numerical values for SMA material parameters are based on values given by the company 'Intrinsic Devices Inc.' San Francisco. For the sake of simplicity, a constant value for Young's modulus E_S was chosen for both phases (martensite and austenite). The Young's modulus E_{st} and yield strength for steel were measured on the Zwick Z050 tensile test machine and the other steel material parameters are taken from materials science handbooks. Radii of both rings were measured on the DEA (Digital electronic automation) coordinate measuring machine (error ±2μm). Input values are presented in Table 1:

Table 1. Input values for numerical calculation of constrained recovery

$a_0 = 9.143$ mm	$b_0 = 16.08$ mm	$A_S = 50$ °C	$A_f = 80$ °C
$T_0 = T_{END} = 20$ °C	$\alpha_S = 1.1\times10^{-5}$ K^{-1}	$\alpha_{st} = 1.15\times10^{-5}$ K^{-1}	$C = 5.5$ MPa/K
$\nu_{st} = 0.3$	$\nu_S = 0.3$	$E_{st} = 195$ GPa	$E_S = 30$ GPa

One SMA ring (a_1 = 9.7015mm and b_1 = 16.515mm, martensite structure) was heated in teflon oil to temperature 89°C for 10 minutes and then cooled down to ambient temperature T_0 = 20°C. No mechanical obstacle (steel ring) was used during this temperature cycle (free recovery). The inner and outer radius of SMA ring a_0 and b_0 were measured at T_0 (austenite structure): a_0 = 9.143mm and b_0 = 16.08mm. These values are used in the model as radii before the 'widening' process. Dimensions of six SMA rings and six steel rings, are shown in Table 2:

Table 2. Dimensions of SMA and steel rings

	a_1 [mm]	b_1 [mm]	c_0 [mm]	d_0 [mm]
1	9.7015	16.514	8.285	9.2035
2	9.7165	16.5155	7.7205	9.252
3	9.711	16.516	7.2145	9.302
4	9.712	16.5145	7.2135	9.2995
5	9.707	16.515	6.9795	9.3525
6	9.708	16.5155	6.999	9.4035

The outer radius of the steel ring d_0 in Table 2 was chosen to contact the SMA ring at different contact temperatures T_C. The width of all SMA and steel rings was the same: 13.75mm. Since biaxial stress state is assumed, the width has no influence on results. The system SMA ring – steel ring was heated in teflon oil few degrees above calculated temperature T_{SE} for 10 minutes and then cooled down to the end temperature which was equal to the ambient temperature: $T_{END} = T_0$ = 20°C. The inner diameters of the steel ring $2c_{end}$ were measured then by the DEA coordinate measuring machine (error ±2μm) and were also calculated numerically, see Table 3. The theoretical radial displacement u^{st}_{the} at inner radius c_0 in Table 3 is calculated from expression $u^{st}_{the} = c^{the}_{end} - c_0$ and the measured one from expression $u^{st}_{\exp} = c^{\exp}_{end} - c_0$. The error in Table 3 is calculated using expression $err = 100(u^{st}_{the} - u^{st}_{\exp}) / u^{st}_{\exp}$. Figure 2 presents the relationship between the theoretical and experimental contact pressures at temperature T_{END} and the outer radii of steel rings d_0. The experimental contact pressures were not measured but were calculated from the measured radial displacements $u^{st}_{\exp}$ from Table 3. From Fig. 2 and Table 3 it can be clearly seen that the comparison between theory and experiment shows a good agreement for the first four examples when stresses are lower. In the model, plastic strains in SMA rings are neglected, but at higher stresses this assumption is not good enough.

Table 3. Theoretical and experimental values of inner diameter $2c$ and radial displacements at inner diameter $2u^{st}$ of steel rings

	T_C [°C]	$2c^{the}_{end}$ [mm]	$2c^{\exp}_{end}$ [mm]	$2u^{st}_{the}$ [μm]	$2u^{st}_{\exp}$ [μm]	error [%]
1	76.73	16.538	16.532	-32	-38	-15.8
2	74.28	15.403	15.403	-38	-38	0
3	71.58	14.387	14.390	-42	-39	7.7
4	71.73	14.386	14.385	-41	-42	-2.4
5	68.84	13.910	13.919	-49	-40	22.5
6	66.15	13.937	13.954	-61	-44	38.6

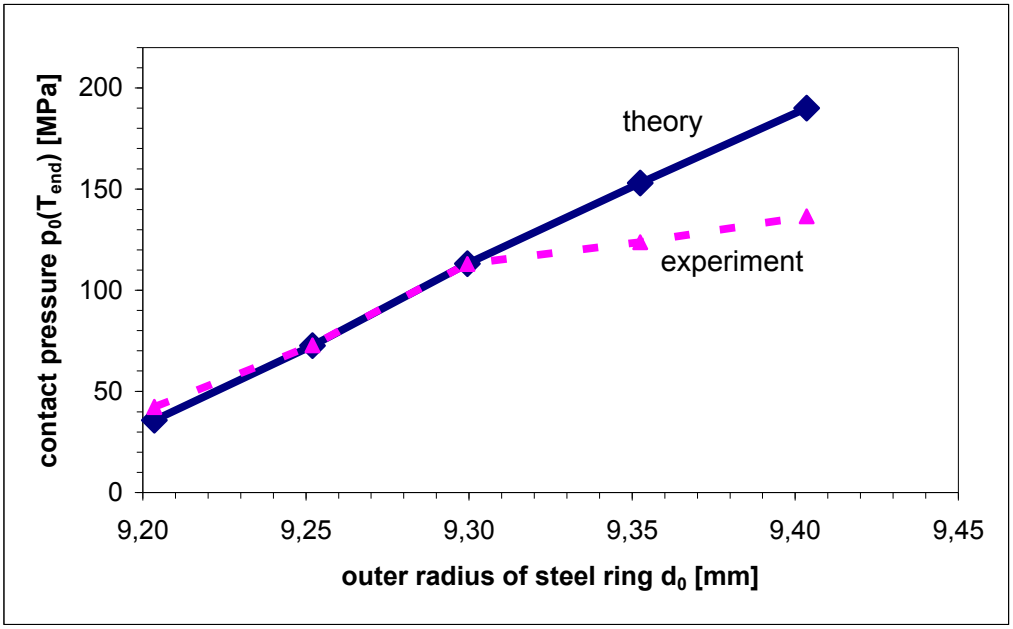

Fig. 2. Experimental and theoretical values of contact pressure versus outer radius d_0 of steel rings

References:

[1] Borden T., Shape-Memory Alloys: Forming a Tight Fit, *Mechanical Engineering*, 113(10), 1991, pp. 67-72.

[2] Kapgan M. and Melton K.N., Shape Memory Alloy Tube and Pipe Couplings, In: *Engineering Aspects of Shape Memory Alloys*, Butterworth-Heinemann, 1990.

[3] Auricchio F., Shape-memory Alloys: Applications, Micromechanics, Macromodelling and Numerical Simulations, Ph.D. thesis, University of California at Berkeley, 1995.

[4] Auricchio F. and Lubliner J., A Uniaxial Model for Shape-memory Alloys, *International Journal of Solids and Structures*, 34(27), 1997, pp. 3601-3618.

[5] Lubliner J. and Auricchio F., Generalized Plasticity and Shape-memory Alloys, *International Journal of Solids and Structures*, 33(7), 1996, pp. 991-1003.

[6] Panoskaltsis V.P., Bahuguna S. and Soldatos D., On the Thermomechanical Modeling of Shape Memory Alloys, *International Journal of Non-linear Mechanics*, 39(5), 2004, pp. 709-722.

[7] Brinson L.C., One-dimensional Constitutive Behavior of Shape Memory Alloys: Thermomechanical Derivation with Non-constant Material Functions and Redefined Martensite Internal Variable, *Journal of Intelligent Material Systems and Structures*, 4, 1993, pp. 229-242.

[8] Kato H., Inagaki N. and Sasaki K., A One-Dimensional Modelling of Constrained Shape Memory Effect, *Acta Materialia*, 52(11), 2004, pp. 3375-3382.

[9] Kosel F. and Videnic T., Generalized Plasticity and Uniaxial Constrained Recovery in Shape Memory Alloys, *Mechanics of Advanced Materials and Structures*, 14(1), 2007, pp. 3-12.

[10] Leclercq S. and Lexcellent C., 1996. A General Macroscopic Description of the Thermomechanical Behavior of Shape Memory Alloys, *Journal of the Mechanics and Physics of Solids*, 44(6), 1996, pp. 953-980.

[11] Stalmans R., Delaey L. and Van Humbeeck J., Generation of Recovery Stresses: Thermodynamic Modelling and Experimental Verification, *Journal de Physique IV*, C5, 1997, pp. 47-52.

[12] Stalmans R., Van Humbeeck J and Delaey L., 1995. Thermodynamic Modelling of Shape Memory Behaviour: Some Examples, *Journal de Physique IV*, C8(5), 1995, pp. 203-208.

[13] Novak V. and Šittner P., Micromechanics Modelling of NiTi Polycristalline Aggregates Transforming Under Tension and Compression Stress, *Materials Science and Engineering A*, 378, 2004, pp. 490-498.

[14] Mohamed H.A., Determination of the Recovery Stresses Developed by Shape Memory Alloys, *Journal of Materials Science*, 13, 1978, pp. 2728-2730.

[15] Otsuka K. and Wayman C.M., 1998. *Shape memory materials*, Cambridge University Press, 1998.

[16] Videnic T., Constrained Recovery in Mechanical Elements Made of Shape Memory Material, Ph.D. thesis, (in Slovene), University of Ljubljana, 2004.